

**Central Arctic Ocean paleoceanography from ~50 ka to present,
on the basis of ostracode faunal assemblages from SWERUS 2014
expedition**

Laura Gemery¹, Thomas M. Cronin¹, Robert K. Poirier^{1&2}, Christof Pearce^{3,4}, Natalia Barrientos³, Matt O'Regan³, Carina Johansson³, Andrey Koshurnikov,^{5,6} Martin Jakobsson³

¹ U.S. Geological Survey, Reston, Virginia

² Rensselaer Polytechnic Institute, Department of Earth & Environmental Sciences, Troy, New York

³ Department of Geological Sciences and Bolin Centre for Climate Research, Stockholm University, Stockholm, 10691, Sweden

⁴ Department of Geoscience, Aarhus University, Aarhus, 8000, Denmark

⁵ Tomsk National Research Polytechnic University, Tomsk, Russia

⁶ Moscow State University, Geophysics, Russian Federation

Correspondence to: Laura Gemery (lgemery@usgs.gov)

Keywords: Arctic Ocean, Quaternary, Sea-ice history, Sediment cores, Paleobiological proxies, Benthic ostracode assemblages

Abstract

Late Quaternary paleoceanographic changes at the Lomonosov Ridge, central Arctic Ocean, were reconstructed from multicore and gravity cores recovered during the 2014 SWERUS-C3 Expedition. Ostracode assemblages dated by accelerator mass spectrometry (AMS) indicate changing sea-ice conditions and warm Atlantic Water (AW) inflow to the Arctic Ocean from ~50 ka to present. Key taxa used as environmental indicators include *Acetabulastoma arcticum* (perennial sea ice), *Polycope* spp. (variable sea ice margins, high surface productivity), *Krithe hunti* (Arctic Ocean deep water), and *Rabilimis mirabilis* (nutrient, AW inflow). Results indicate periodic seasonally sea-ice free conditions during Marine Isotope Stage (MIS) 3 (~57-29 ka), rapid deglacial changes in water mass conditions (15-11 ka), seasonally sea-ice free conditions during the early Holocene (~10-7 ka) and perennial sea ice during the late Holocene. Comparisons with faunal records from other cores from the Mendeleev and Lomonosov Ridges suggest generally similar patterns, although sea-ice cover during the last glacial maximum may have been less extensive at the new Lomonosov Ridge core site (~85.15°N, 152°E) than farther north and towards Greenland. The new data provide evidence for abrupt, large-scale shifts in ostracode species depth and geographical distributions during rapid climatic transitions.

1. Introduction

Environmental conditions are changing rapidly in the Arctic Ocean today, but a longer time perspective is necessary to assess and contextualize these changes and their contributing factors. These changing conditions include sea ice extent and thickness (Stroeve et al., 2012, 2014; Laxon et al., 2013), as well as ocean temperature, stratification, circulation, chemistry, and ecology (Polyakov et al, 2017; Moore et al, 2015; Chierici and Fransson 2009; Rabe et al., 2011;

Grebmeier et al., 2006, 2012; Wassmann et al., 2011). Sea ice extent and thickness, in particular, are challenging parameters to reconstruct because most sea ice proxies lack temporal and geographical resolution (Stein et al., 2012). Sea ice extent and thickness, however, are very important variables because they influence albedo, near-surface salinity, light levels, surface-to-seafloor organic carbon flux, and other variables that are important to ecosystems. In fact, sea ice exerts a primary control on Arctic biological and geochemical cycles (Anderson et al., 2011), and sea ice changes are in part responsible for fast-feedback climate changes during the geologic past (Polyak et al., 2010).

Before the last few decades, instrumental oceanographic records were relatively sparse, and sediment proxy records provided insight into past sea-ice conditions and ocean circulation changes from all regions of the Arctic. These records are especially important for examining sea-ice history during past climate changes before the availability of instrumental records. The composition and abundance of marine microfossils preserved in many Arctic sediments provide an important constituent that helps address the growth and decay of ice sheets. For example, several excursions in records of oxygen and carbon isotopes of planktic foraminifers from Arctic sediment cores have been interpreted as releases of freshwater from collapsing continental ice sheets during glaciations and glacial terminations (Stein et al., 1994; Nørgaard-Pedersen et al., 1998)

This paper examines temporal changes in microfossil shells from ostracode indicator species that shed light on biological productivity and sea-ice extent during the last ~50 ka, including Marine Isotope Stages (MIS) 3, the Last Glacial Maximum (LGM, ~21 ka), the deglacial interval and the Holocene. Ostracoda are bivalved Crustacea that inhabit Arctic marine habitats and whose assemblages (Cronin et al., 1994, 1995, Poirier et al., 2012) and shell chemistry (Cronin et al., 2012) have been used extensively as proxies to reconstruct Arctic paleoceanography and sea-ice history (Cronin et al., 2010). Most ostracode species are benthic in habitat and their ecology reflects bottom water environmental conditions. Benthic ecosystems rely on biological productivity in the upper water column, and so benthic biomass production and community structure also reflect sea-ice cover and surface-to-bottom ecosystem links (Grebmeier and Barry, 1991; Grebmeier et al., 2006).

Two pelagic/epipelagic ostracode taxa are used in this paper to indicate water mass conditions. Sediment cores for this study were collected during the 2014 SWERUS-C3 (Swedish – Russian – US Arctic Ocean Investigation of Climate-Cryosphere-Carbon Interactions) Leg 2 expedition from previously unstudied regions of the Siberian margin and the Lomonosov Ridge. The radiocarbon-dated records presented here are from 85.15°N, 152°E on the Lomonosov Ridge in the central Arctic Ocean, a site located at ~800 m near the transition between Atlantic Water and Arctic Intermediate Water in the modern Arctic Ocean. During prior glacial-interglacial cycles, the region was influenced to various degrees by the strength and depth penetration of Atlantic Water. For example, during glacial intervals when thick ice shelves covered much of the Arctic Ocean (Jakobsson et al., 2016), Arctic Intermediate Water warmed (Cronin et al., 2012) and likely entrained to greater water depths (Poirier et al., 2012). Consequently, the new

results, when compared to published faunal records from other regions of the Arctic Ocean (Fig. 1a, Table 1), show some regional differences but an overall remarkable consistency in central Arctic faunal abundance changes during the late Quaternary.

2. Arctic oceanography

The Arctic Ocean is strongly stratified, with distinct water masses separated by vertical changes in salinity and temperature (Figure 1b). The following summary of Arctic water masses and circulation is taken from Aagaard and Carmack (1989), Anderson et al. (1994), Jones (2001), Olsson and Anderson (1997), Rudels et al. (2012 and 2013). Arctic Ocean water masses include a fresh, cold Polar Surface Water layer ([PSW], $T = \sim 0^{\circ}\text{C}$ to -2°C , $S = \sim 32$ to 34), found between ~ 0 and 50 m. The PSW is characterized by perennial ice in most regions and seasonal sea ice in the margins of the Arctic Ocean. Beneath the sea-ice cover, a strong halocline separates the PSW from the underlying warmer, denser water mass of North Atlantic origin (Atlantic Water [AW], ~ 200 to 1000 m, $T = > 0^{\circ}\text{C}$, $S = \sim 34.6$ to 34.8). One branch of the AW flows into the Arctic Ocean from the Nordic seas along the eastern Fram Strait off the west coast of Spitsbergen and another branch flows through the Barents Sea. An intermediate-depth water mass below the AW in the Eurasian Basin at ~ 1000 - 1500 m is called the Arctic Intermediate water ([AIW], $T = -0.5$ to 0°C , $S = \sim 34.6$ to 34.8). Below 2000 m, the deep Arctic basins are filled with Arctic Ocean Deep Water ([AODW], $T = -1.0^{\circ}\text{C}$ to -0.6°C , $S = 34.9$, Somavilla et al., 2013). Bathymetry is a dominant factor governing circulation patterns for AW and AIW, and a sharp front over the Lomonosov Ridge near the SWERUS-C3 core site studied here partially isolates these waters in the Eurasian Basin from the Canadian Basin (Fig. 1b).

In addition to Arctic Ocean stratification, other factors influence sea-ice decay and growth over geologic time (i.e. Polyak et al., 2010). A recent study by Stein et al. (2017) notes the importance of large-scale atmospheric circulation patterns, such as the North Atlantic Oscillation (NAO) and Arctic Oscillation (AO), and radiative forcing (i.e. solar activity) on Holocene sea ice thickness, extent and duration. The NAO and AO influence changes of the relative position and strength of the two primary Arctic Ocean surface-current systems, the Beaufort Gyre in the Amerasian Basin and the Transpolar Drift in the Eurasian Basin (Fig. 1a; Rigor et al., 2002; Stroeve et al., 2014). Data resulting from the SWERUS expedition will help improve understanding of the spatial patterns of sea-ice and intermediate depth circulation, given the extreme variability in sea ice in this region recently evident from satellite records (Serreze and Stroeve, 2015; Stroeve et al., 2014), the importance of the Transpolar Drift in sea ice export through Fram Strait (Polyak et al., 2010; Smedsrud et al., 2017) and new evidence for the influence of inflowing Atlantic Water on sea ice and “atlantification” of the Eurasian Basin (Polyakov et al. 2017).

3. Materials and methods

3.1 Core material and sample processing

Cores for this study were obtained during the September 2014 SWERUS-C3 (Leg 2) expedition to the eastern Arctic Ocean aboard Swedish Icebreaker *Oden*. Figure 1 shows the location of multicore SWERUS-L2-32-MC4 (85.14°N, 151.57°E, 837 m) and nearby gravity core SWERUS-L2-32-GC2 (85.15°N, 151.66°E, 828 m) on the Lomonosov Ridge. These cores are hereafter referred to as 32-MC and 32-GC, respectively. Both cores were stored at 4°C and sampled at the Department of Geological Sciences, Stockholm University. Processing of the samples involved washing the sediment with water through a 63-µm mesh sieve. Core 32-MC was processed in Stockholm while 32-GC was processed at the U.S. Geological Survey (USGS) laboratory in Reston, Virginia. Sediment samples (1-cm thick, ~30 g prior to processing) were taken every centimeter in 32-MC along its 32 cm length. Section 1 (117 cm) of 32-GC was sampled every 2-3 cm (2-cm thick, ~45-60 g wet weight).

After processing and oven drying the samples, the residual >125 µm size fraction was sprinkled on a picking tray and ostracodes were removed to a slide. One exception for expediency is that specimens of the genus *Polycope* were counted and not removed from the sediment. A total of ~300 specimens were studied from each sample of 32-MC. More detailed counts of some samples in 32-MC were done periodically, where all specimens were picked and/or counted to ensure that 300 specimens provided a representative assemblage. In 32-GC, all specimens were picked and/or counted in each sample. Ostracodes were present throughout the entire studied intervals of both 32-MC and down to 62 cm in 32-GC. Planktic and benthic foraminifers were also present in abundance but not studied.

3.2 Chronology, reservoir corrections and sedimentation

Nine radiocarbon (^{14}C) ages were obtained from core 32-MC using accelerator mass spectrometry (AMS) (Fig. 2, Table 2). Most dates were obtained on mollusks (*Nuculidae* and *Arcidae* spp.), except a few samples where mollusks and benthic foraminifera were combined. Two ages from 32-GC were obtained using a combination of mollusks, foraminifera and ostracode shells. The final age models representing the two cores combined are based on all the calibrated ^{14}C ages listed in Table 2. Generally, ages >40 ka should be considered with caution because of large uncertainties in the radiocarbon calibration curve and high sensitivity to even extremely small levels of contamination. Calibration into calendar years was carried out using Oxcal4.2 (Bronk Ramsey, 2009) and the Marine13 calibration curve (Reimer et al., 2013), using a local marine reservoir correction, ΔR , of 300 ± 100 years. Because ΔR values for the central Arctic Ocean were not constant during the last 50 ka, it is difficult to date pre-Holocene sediments independently (Pearce et al., 2017; Hanslik et al., 2012), and improved age models may be available in the future.

Patterns in ostracode assemblages in both cores were used to correlate cores 32-MC and 32-GC and produce a composite faunal record, which led to a 3-cm offset for core 32-GC. After adding the 3-cm offset to sample depths of 32-GC, the 32-MC core chronology was applied down to 31.5 cm core depth (dated at 39.6 ka). The average sedimentation rate at the core site was ~1.5 cm/ka, which is typical of central Arctic Ocean ridges (Backman et al., 2004; Polyak et al., 2009).

The lower section of 32-GC, from 31.5 cm to 61 cm, is beyond the limit of radiocarbon dating. However, the litho-stratigraphy of the gravity core can be readily correlated to other records from the central Lomonosov Ridge, where multiple dating techniques constrain the approximate positions of MIS 4 and 5 boundaries (Jakobsson et al., 2001; O'Regan, 2011). A correlation between SWERUS-C3 32-GC and AO96/12-1PC was previously presented in Jakobsson et al. (2016). The correlation is supported by the occurrences in 32-GC of the calcareous nannofossil *E. huxleyii* (Fig. 2). Based on this longer-term correlation, sediments between 31 and 61 cm are less than 50 ka. This age estimate is consistent with previous work on the Lomonosov Ridge, revealing a prominent transition from coarse-grained, microfossil-poor sediments (diamict) into bioturbated, finer-grained, microfossiliferous sediments that occurred during MIS 3 at approximately 50 ka (Spielhagen et al., 2004; Nørgaard-Pederson et al., 2007).

4. Results and Discussion

4.1 Ostracode taxonomy and ecology

The SWERUS 32 cores contained a total of 13,767 ostracode specimens in 32-MC and a total of 5,330 specimens in the uppermost 5-62 cm of 32-GC (the top few centimeters below the seafloor were not recovered in the gravity core). The bottom 54 cm of 32-GC (section 1 from 63-117 cm) was barren of calcareous material. Twenty-eight ostracode species were identified in 32-MC and 21 species were identified in 32-GC. Supplementary Tables S1 and S2 provide all species and genus census data for 32-MC and 32-GC, respectively. Data will also be accessible at NOAA's National Centers for Environmental Information (NCEI, <https://www.ncdc.noaa.gov/paleo-search/>). The primary sources of taxonomy and ecology were papers by Cronin et al. (1994, 1995, 2010), Gemery et al. (2015), Joy and Clark (1977), Stepanova (2006), Stepanova et al. (2003, 2007, 2010), Whatley et al. (1996, 1998), and Yasuhara et al. (2014).

Podocopid ostracodes were identified at the species level except the genera *Cytheropteron* and myodocopid *Polycope*. Table 3 provides a list of species included in the genus-level groups, which was sufficient to reconstruct paleoenvironmental changes. There are several species of *Cytheropteron* in the deep Arctic Ocean but they are not ideal indicator species given their widespread modern distributions. There are at least eight species of *Polycope* in the Arctic Ocean, but juvenile molts of *Polycope* species are difficult to distinguish from one another. Most specimens in 32-MC and 32-GC belonged to *P. inornata* Joy & Clark, 1977 and *P. bireticulata* Joy & Clark, 1977. Nonetheless, most *Polycope* species co-occur with one another, are opportunistic in their ecological strategy, and dominate assemblages associated with high surface productivity and organic matter flux to the bottom (Table 4; Karanovic and Brandão, 2012, 2016).

The relative frequency (percent abundance) of individual dominant taxa is plotted in Figure 3 and listed in Supplementary Table S3. Abundances were computed by dividing the number of individual species found in each sample by the total number of specimens found. For 32-MC, using the algorithm for a binomial probability distribution provided by Raup (1991), ranges of uncertainty ("error bars") were calculated at the 95% fractile for the relative frequency in each sample to the relative frequency of each species and the total specimen count of each sample at

a given core depth (Supplementary Table S4). Faunal densities were high enough to allow comparisons from sample to sample, and Supplementary Table S4 lists the density of ostracode specimens per gram of dry sediment, which averaged >125 shells per gram sediment. For this study of the SWERUS-C3 32 cores, the focus was on an epipelagic species (*Acetabulastoma arcticum*), a pelagic genera (*Polycope* spp.), three benthic species (*Krithe hunti*, *Pseudocythere caudata*, *Rabilimis mirabilis*) and a benthic genus (*Cytheropteron* spp.). Table 4 provides an overview of pertinent aspects of these species' ecology that have paleoceanographic application.

4.2 Temporal patterns in ostracode indicator species from SWERUS-C3 32-MC/GC

The faunal patterns in cores from the SWERUS-C3 32-MC/GC sites confirm faunal patterns occurring over much of the central Arctic Ocean during the last 50 ka, including MIS 3-2 (~50 to 15 ka), the last deglacial interval (~15 to 11 ka), and the Holocene (~11 ka to present). Similar patterns are seen in both the multicore and gravity core. Relative frequencies of indicator taxa in cores 32-MC and 32-GC (Fig. 3) show four distinct assemblages, which are referred to as informal faunal zones following prior workers (Cronin et al., 1995; Poirier et al., 2012). These zones are as follows: (1) *Krithe* zone (primary abundance up to 80% during ~45-42 ka and a secondary abundance of 5-10% during ~42-35 ka); (2) *Polycope* zone (with abundance of 50 to 75% during ~40-12 ka, also containing a double peak in abundance of *P. caudata*); (3) *Cytheropteron-Krithe* zone (12-7 ka); and (4) *Acetabulastoma arcticum* zone (~7 ka-present). This paper briefly discusses the paleoceanographic significance of each period in the following sections 4.3 - 4.5 based on the comparison cores presented in Figs 4 and 5. Figures 4 and 5 compare the new SWERUS-C3 results from 32-MC with published data from box and multicores from the Lomonosov and Mendeleev Ridges, respectively, covering a range of water depths from 700 m to 1990 m. Most records extend back to at least 45 ka, and the age model for each core site is based on calibrated radiocarbon ages from that site (i.e. Cronin et al., 2010, 2013; Poirier et al., 2012). In addition, section 4.6 discusses a potential new indicator species, *R. mirabilis*, which exhibits distinct faunal migrations that coincide with *Krithe* zones in 32-MC/GC. *R. mirabilis* lives on today's continental shelf but is found in limited intervals in sediment cores that are far outside its usual depth and geographic range. *R. mirabilis* migrations are documented not only in 32-MC/GC but in cores 96-12-1PC, HLY0503-06JPC, P1-94-AR-PC10, P1-92-AR-PC40, LOMROG07-04 and P1-92-AR-PC30.

4.3 MIS 3-2 (~50-15 ka)

A strong peak in the abundance of *Krithe hunti* (Fig. 3) is seen in 32-GC sediments estimated to be ~45-42 ka in age. A similar peak of lower but still significant abundance also occurs in sediments dated between 42 and 35 ka, and this peak is consistent with other cores on the Mendeleev Ridge and particularly on the Lomonosov Ridge (Figs 4, 5). Prior studies of Arctic ostracodes have shown that *Krithe* typically signifies cold well-ventilated deep water and perhaps low food supply (Poirier et al., 2012 and references therein). *Krithe* is also a dominant component (>30%) of assemblages in North Atlantic Deep Water (NADW) in the

subpolar North Atlantic Ocean. Its abundance varies during glacial-interglacial cycles, reaching maxima during interglacial and interstadial periods (Alvarez Zarikian et al., 2009). Peaks in the abundance of *Krithe* in the Arctic Ocean probably signify faunal exchange between the North Atlantic Ocean and the Greenland-Norwegian Seas through the Denmark Strait and Iceland Faroes Ridge and the central Arctic through the Fram Strait. In other Arctic Ocean cores, the ostracode genus *Henryhowella* is often associated with *Krithe* sp. in sediments dated between ~50 to 29 ka (MIS 3), and its absence in the 32-MC/GC cores may reflect the relatively shallow depth at the coring site. While *Henryhowella* was absent in records from this site, *R. mirabilis* abruptly appears and spikes to an abundance of 60 percent at 40 ka, which coincides with the *Krithe* zone.

A. arcticum is present in low abundance (~5%) in sediment dated at ~42 to 32 ka in 32-MC/GC (Fig. 3), signifying intermittent perennial sea ice. A second increase in abundance of *A. arcticum* corresponds to a (modeled, mean, 2-sigma) radiocarbon date of 21.6 ka. This suggests the location of this core may not have been covered by thick ice during the LGM as long as other areas.

A *Krithe* to *Polycope* shift occurred at ~35-30 ka. This “K-P shift” is a well-documented, Arctic-wide transition (Cronin et al., 2014) that has paleoceanographic significance as well as biostratigraphic utility. *Polycope* is clearly the dominant genus group from sediment dated ~40-12 ka in 32-MC/GC and all sites on the Lomonosov and Mendeleev Ridges (Figs. 4, 5), signifying high productivity likely due to an intermittent, rapidly oscillating sea-ice edge at the surface. *P. caudata* has varying percentages (3-14%) in sediment dated ~40-12 ka, depending on the site. *P. caudata* is an indicator of AI water and Cronin et al. (2014) report that it appears to be ecologically linked to the surface conditions. *Cytheropteron* spp. is present in moderate abundance (20-30%) in sediment dated ~35-15 ka.

Overall, the faunal characteristics from this time period imply relatively restricted and/or poorly ventilated intermediate waters near the 32-MC/GC site. The major exception to this corresponds with the pronounced peaks in *Krithe* and *R. mirabilis*. This significant shift in faunal composition implies changes in ice margins, AW inflow, deep ocean ventilation and/or enhanced deep-water transfer between the Central Arctic Ocean and the North Atlantic.

4.4 The Last Deglacial Interval (~15 to 11 ka)

The major shift from *Polycope*-dominated to *Cytheropteron-Krithe*-dominated assemblages occurs in sediment dated 12 ka in 32-MC/GC and ~15-12 ka in other Lomonosov and Mendeleev Ridge cores. In 32-MC/GC, *Krithe* reappears in low (10%) but significant abundance after 11 ka after being absent during MIS 2. Both *Cytheropteron* and *Krithe* are typical faunas in NADW. Although low sedimentation rates prevent precise dating of this shift, it almost certainly began ~14.5 ka at the Bølling-Allerød warming transition. Because the Bering Strait had not opened yet (Jakobsson et al., 2017), this faunal shift must have been related to one or several of the following changes: (1) atmospheric warming; (2) strong Atlantic Water inflow through the Barents Sea; and (3) strong Atlantic Water inflow through the eastern Fram Strait. *A. arcticum* is absent or rare (<2% of the assemblage) in sediment

dated ~15-12 ka, suggesting minimal perennial sea ice cover and probably summer sea-ice free conditions during late deglacial warming.

4.5 The Holocene (~11 to Present)

Krithe and *Cytheropteron* remain abundant in sediment dated ~10-7 ka (early Holocene) across most of the central Arctic Basin, signifying continued influence of water derived from the North Atlantic Ocean (Figs. 4, 5). Also during this time, *R. mirabilis* reappears and spikes to an abundance of 55 percent at ~8 ka. *A. arcticum* (which represents the *A. arcticum* zone) increases to >6-8% abundance beginning in sediment dated ~7 ka, and increases to >10% abundance in sediment dated ~3 ka. This increase in abundance is correlated with an increase in perennial-sea ice, and is more prominent in cores from the Lomonosov Ridge than in cores from the Mendeleev Ridge (most likely due to more persistent perennial sea ice cover over the Lomonosov Ridge sites). The inferred middle to late Holocene development of perennial sea ice is consistent with interpretations from other sea-ice proxies (Xiao et al., 2015) and with the transition from an early-middle Holocene “thermal maximum” (Kaufman et al., 2004, 2016) to cooler conditions during the last few thousand years.

4.6 *Rabilimis mirabilis*: New faunal events signifying rapid oceanographic change

In addition to the standard ostracode zones discussed above, the cores from the SWERUS 2014 expedition provide evidence of uncharacteristic and brief, yet significant events of faunal dominance of a taxon. Such events are indicative of rapid environmental change. For example, prior studies have documented range shifts in Arctic benthic foraminifera during the last deglacial and Holocene intervals from the eastern Arctic Ocean (Wollenburg et al., 2001), the Laptev Sea (Taldenkova et al., 2008, 2012), the Beaufort Sea and Amundsen Gulf (Scott et al., 2009) and in older sediments (Polyak et al., 1986, 2004; Ishman et al., 1996; Cronin et al., 2014). The SWERUS-32 data reveal two *Rabilimis mirabilis* “events” – intervals containing high proportions of this shallow water ostracode species dated at ~45-36 ka and 9-8 ka. The modern circum-Arctic distribution of *R. mirabilis* is confined to shallow (<200 m) water depths (Fig. 6a, b, and c; Hazel, 1970; Neale and Howe, 1975; Taldenkova et al., 2005; Stepanova, 2006; Gemery et al., 2015). *R. mirabilis* can also tolerate a range of salinities, explaining its presence in regions near river mouths with reduced salinity (Fig. 6a). *R. mirabilis* also occurs in 2014 SWERUS-C3 multicore top samples on the Eastern Siberian Sea slope (Supplementary Table S5; cores 23-MC4 (4%, 522 m); 18-MC4 (18%, 349 m); 16-MC4 (11%, 1023 m); 15-MC4 (41%, 501 m) and 14-MC4 (70%, 837 m). These locations correspond to the summer sea-ice edge that has receded during recent decades over the Lomonosov Ridge.

Figures 7a and 7b show the stratigraphic distribution of *R. mirabilis* at the new SWERUS site and other sites on the Lomonosov Ridge (96-12-1PC), the Mendeleev Ridge (P1-94-AR-PC10) and Northwind Ridge (P1-92-AR-PC40) and in longer cores on the Lomonosov and Northwind Ridge. These patterns suggest a depth range extension of *R. mirabilis* into deeper water (700 to 1673 m) during interstadial periods (MIS 5c, 5a, 3). The abundance of *R. mirabilis* reaches 40-50% of the total assemblage at Lomonosov Ridge site 96-12-1PC at a water depth of 1003 m. Such anomalously high percentages of well-preserved adult and

juvenile specimens of *R. mirabilis* indicate that they were not brought to the site through sediment transport from the shelf. Instead, the *R. mirabilis* events represent in-situ populations. Although these *R. mirabilis* events are not synchronous, most occur in sediment dated ~96-71 ka (late MIS 5) and at SWERUS-C3 sites of 32-MC and 32-GC in sediment dated 45-36 ka and ~9-8 ka (early Holocene). Thus the *R. mirabilis* events correlate with interglacial/interstadial periods that experienced summer sea-ice free and/or sea-ice edge environments where there may have been enhanced flux of surface-to-bottom organic matter. However, additional study of cores from Arctic margins will be required to confirm the paleoceanographic significance of *R. mirabilis* migration events.

5. Conclusions

Changes in ostracode assemblages in new cores from the central Arctic Ocean signify major paleoceanographic shifts at orbital and suborbital scales during the last 50 ka. Peaks in dominant ostracode taxa include: (1) *Krithe* zone (~45-35 ka); (2) *Polycopse* zone (~40-12 ka); (3) *Cytheropteron-Krithe* zone (~12-7 ka); and (4) *Acetabulastoma arcticum* zone (~7 ka-present). Brief yet significant depth migrations of *R. mirabilis* corresponding with the *Krithe* zone and *Cytheropteron-Krithe* zone imply rapid paleoceanographic changes associated with influx of Atlantic Water and/or deep ocean convection during suborbital events in MIS 3 and the late deglacial to early Holocene. When ostracode assemblage patterns in 32-MC/GC cores are compared to similar records from the Northwind, central Lomonosov, Mendeleev and Gakkel Ridges (Cronin et al., 1995, 2010, Poirier et al., 2012), these changes demonstrate pan-Arctic, nearly synchronous changes in benthic ecosystems in association with rapid sea ice, surface productivity, and oceanographic changes in the Atlantic Water and Arctic Intermediate Water during MIS 3-1 (the last 50 ka). These results confirm the sensitivity of Arctic benthic fauna to large, sometimes abrupt, climate transitions.

Acknowledgements

We are grateful to the crew of Icebreaker *Oden* and the SWERUS-C3 Scientific Team. Thanks to A. Ruefer for assistance with sample processing. This manuscript benefitted from reviews by X. Crosta, A. de Vernal, C. Swezey and M. Toomey. This study was funded by the U.S. Geological Survey Climate R&D Program. Any use of trade, firm, or product names is for descriptive purposes only and does not imply endorsement by the U.S. Government. A. Koshurnikov acknowledges financial support from the Russian Government (grant number 14, Z50.31.0012/03.19.2014). Data presented in the article acquired during the 2014 SWERUS-C3 expedition are available through the Bolin Centre for Climate Research database: <http://bolin.su.se/data/>.

Fig 1. a.) International Bathymetric Chart of the Arctic Ocean showing the location of this study's primary sediment cores on the Lomonosov Ridge (red star: 32-GC2 and 32-MC4), and other core sites discussed in this paper (black circles, white

circles). (See Table 1 for supplemental core data.) White circles designate cores that contain *Rabilimis mirabilis* events. Red arrows show generalized circulation patterns of warm Atlantic water in the Arctic Ocean. White arrows indicate the surface flow of the Transpolar Drift, which moves sea ice from the Siberian coast of Russia across the Arctic basin, exiting into the North Atlantic off the east coast of Greenland. Transect line through the map from “1” in the Chukchi Sea to “2” in the Barents Sea shows direction of temperature profile in Fig1b.

b.) Cross section of modern Arctic Ocean temperature profile from showing major water masses. PSW: polar surface water, AL: Atlantic layer, AIW: Arctic intermediate Water, AODW: Arctic Ocean Deep water. Ocean Data View Source: Schlitzer, 2012. Ocean Data View: <http://odv.awi.de>

Fig. 2 Chronology and stratigraphy of SWERUS-32-GC and 32-MC. Bulk density and magnetic susceptibility profiles for 32GC were previously correlated to the well-dated 96-12-1PC core by Jakobsson et al. (2016). Bulk density primarily reflects changes in grain size, with coarser material having a higher density than finer grained material. The overall position of MIS 5 is supported by the occurrence of *E. huxleyi*. The chronology for the upper 30-35 cm is based on radiocarbon dating in both 32-MC and 32-GC. Beyond the range of radiocarbon dating, an extrapolation to the inferred position of MIS 3/4 boundary (57 ka at 105 cm) is applied.

Fig 3. Relative frequencies (percent abundance) of dominant taxa in SWERUS-C3 32-MC and 32-GC. The y-axis shows the modeled, mean age during a 2-sigma range of uncertainty.

Fig 4. Relative frequencies (percent abundance) of dominant taxa in SWERUS 32-MC (dotted line) compared to other Lomonosov Ridge cores 2185, 2179 and AOS94 28 (Poirier et al., 2012). The chronology for core PS 2185-4 MC (1051 m) is described in Jakobsson et al., 2000, Nørgaard-Pederson et al., 2003, Spielhagen et al., 2004; core PS 2179-3 MC (1228 m) in Nørgaard-Pederson et al., 2003 and Poirier et al., 2012; and core AOS94 28 (PI-94-AR-BC28, 1990 m) in Darby et al., 1997.

Fig 5. Relative frequencies (percent abundance) of dominant taxa in SWERUS 32-MC (dotted line) compared to other Mendeleev Ridge cores AOS94 8 (Poirier et al., 2012), AOS94 12, and HLY6. The chronology for core HLY6 (HLY0503-06JPC, 800 m) is described in Cronin et al., 2013; core AOS94 8 (PI-94-AR-BC8, 1031 m) in Cronin et al., 2010 and Poirier et al., 2012; and core AOS94 12A (PI-94-AR-BC12A, 1683 m) in Cronin et al., 2010.

Fig 6. a.) Occurrence map of *Rabilimis mirabilis* in the Arctic Ocean and surrounding seas based on 1340 modern surface samples in the Arctic Ostracode Database (AOD; Gemery et al., 2015).
b.) Modern depth and c.) latitudinal distribution of *R. mirabilis* based on 1340-modern surface samples in the AOD (Gemery et al., 2015).

Fig 7. a.) Relative frequency (percent abundance) of *R. mirabilis* in SWERUS-32 cores and in central Arctic Ocean cores, 160 ka to present. b.) *R. mirabilis* in core LOMROG07-04 from 260 ka to present and in core P1-92-AR-PC30 from 340 ka to present.

References

- Aagaard, K. and Cannack, E.C.: The role of sea ice and other fresh water in the Arctic circulation, *J Geophys Res*, 94(14), 485-498, doi:10.1029/JC094iC10p14485, 1989.
- Anderson, L.G., Olsson, K., Skoog, A.: Distribution of dissolved inorganic and organic carbon in the Eurasian Basin of the Arctic Ocean. In: O. M. Johannessen, R. D. Muench, and J. E. Overland, (eds.), *The Polar Oceans and their Role in Shaping the Global Environment*, Geophysical Monograph 85, American Geophysical Union, 525-562, 1994.
- Anderson, L.G., Björk, G., Jutterström, S., Pipko, I., Shakhova, N., Semiletov, I. and Wählström, I.: East Siberian Sea, an Arctic region of very high biogeochemical activity, *Biogeosciences*, 8(6), 1745–1754, doi:10.5194/bg-8-1745, 2011.
- Backman, J., Jakobsson, M., Lovlie, R., Polyak, L., and Febo, L. A.: Is the central Arctic Ocean a sediment starved basin?, *Quaternary Sci Rev*, 23, 1435-1454, 2004.

- 501 Brady, G. S.: A Monograph of the Recent British Ostracoda, Transact Linn Soc
502 London, 26(2), 353–495, 1868.
- 503 Brady, G.S., Crosskey, H.W., Robertson, D.: A Monograph of the Post-Tertiary
504 Entomostraca of Scotland, Including Species from England and Ireland,
505 Paleontograph Soc London, 28, 1–232, 1874.
- 506 Bronk Ramsey, C.: Bayesian Analysis of Radiocarbon Dates, Radiocarbon, 51(1),
507 337–360, doi:10.2458/azu_js_rc.v51i1.3494, 2009.
- 508 Chierici, M. and Fransson, A.: Calcium carbonate saturation in the surface water of
509 the Arctic Ocean: undersaturation in freshwater influenced shelves,
510 Biogeosciences, 6, 2421-2431, doi:10.5194/bg-6-2421-2009, 2009.
- 511 Cronin, T. M., DeNinno, L. H., Polyak, L., Caverly, E. K., Poore, R. Z., Brenner, A.,
512 Rodriguez-Lazaro, J. and Marzen, R. E.: Quaternary ostracode and foraminiferal
513 biostratigraphy and paleoceanography in the western Arctic Ocean, Mar
514 Micropaleontol, 111, 118-133, 2014.
- 515 Cronin, T.M., Polyak L., Reed, D., Kandiano, E.S., Marzen, R.E., Council, E.A.: A
516 600-ka Arctic sea-ice record from Mendeleev Ridge based on ostracodes,
517 Quaternary Sci Rev, 79, 157-167, 2013.
- 518 Cronin, T.M., Dwyer, G.S., Farmer, J., Bauch, H.A., Spielhagen, R.F., Jakobsson,
519 M., Nilsson, J., Briggs, W.M., Stepanova, A.: Deep Arctic Ocean warming during
520 the Last Glacial cycle, Nat Geosci, 5, 631-634, 2012.
- 521 Cronin, T.M., Gemery, L., Briggs, W.M. Jr., Jakobsson, M., Polyak, L., Brouwers,
522 E.M.: Quaternary Sea-ice history in the Arctic Ocean based on a new Ostracode
523 sea-ice proxy, Quaternary Sci Rev, 1-15, doi:10.1016/j.quascirev.2010.05.024,
524 2010.
- 525 Cronin, T. M., DeMartino, D. M., Dwyer, G. S. and Rodriguez-Lazaro, J.: Deep-sea
526 ostracode species diversity: response to late Quaternary climate change, Mar
527 Micropaleontol, 37, 231-249, 1999.
- 528 Cronin, T.M., Holtz, T.R., Jr., Stein, R., Spielhagen, R., Fütterer, D. and
529 Wollenberg, J.: Late Quaternary paleoceanography of the Eurasian Basin, Arctic
530 Ocean, Paleoceanography, 10(2), 259–281, doi:10.1029/94PA03149, 1995.
- 531 Cronin, T.M., Holtz, T.R., Jr. and Whatley, R.C.: Quaternary Paleoceanography of
532 the deep Arctic Ocean based on quantitative analysis of Ostracoda, Mar Geol,
533 19(3–4), 305–332, doi:10.1016/0025-3227(94)90188-0, 1994.
- 534 Darby, D. A., Bischof, J.F. Jones, G.A: Radiocarbon chronology of depositional
535 regimes in the western Arctic Ocean, Deep-Sea Research, 44, 1745-1757, 1997.

- 536 Feyling-Hanssen, R.W.: Foraminiferal stratigraphy in the Plio- Pleistocene Kap
537 København Formation, North Greenland, Meddelelser om Grønland, Geoscience,
538 24, 1-32, 1990.
- 539 Gemery, L., Cronin, T. M., Briggs Jr, W. M., Brouwers, E. M., Schornikov, E. I.,
540 Stepanova, A., Wood, A. M., and Yasuhara, M.: An Arctic and Subarctic ostracode
541 database: biogeographic and paleoceanographic applications, *Hydrobiologia*, 1-37,
542 2016.
- 543 Grebmeier, J. M.: Shifting Patterns of Life in the Pacific Arctic and Sub-Arctic
544 Seas, *Annu Rev Mar Sci*, 4, 63-78, 2012.
- 545 Grebmeier, J.M., Overland, J.E., Moore, S.E., Farley, E.V., Carmack, E.C.,
546 Cooper, L.W., Frey, K.E., Helle, J.H., McLaughlin, F.A. and McNutt, S.L.: A major
547 ecosystem shift in the northern Bering Sea, *Science*, 311(5766),1461-1464, doi:
548 [10.1126/science.1121365](https://doi.org/10.1126/science.1121365), 2006.
- 549
550 Hazel, J.E.: Atlantic continental shelf and slope of the United States-ostracode
551 zoogeography in the southern Nova Scotian and northern Virginian faunal
552 provinces, U.S. Geological Survey Professional Paper, 529-E, E1-E21, 1970.
- 553 Ishman, S. E. and Foley, K. M.: Modern benthic foraminifer distribution in the
554 Amerasian Basin, Arctic Ocean, *Micropaleontology*, 42, 206-220, 1996.
- 555 Jakobsson, M., Pearce, C., Cronin, T.M., Backman, J., O'Regan, M., Anderson,
556 L.G., Barrientos, N., Björk, G., Coxall, H., Mayer, L.A., Mörrh, C.-M., Nilsson, J.,
557 Rattray, J.E., Stranne, C., Semiletov, I.: Post-glacial flooding of the Beringia Land
558 Bridge dated to 11,000 cal yrs BP based on new geophysical and sediment record,
559 *Climate of the Past*, this issue, 2017.
- 560 Jakobsson, M., Nilsson, J., Anderson, L.G., Backman, J., Bjork, G., Cronin, T.M.,
561 Kirchner, N., Koshurnikov, A., Mayer, L., Noormets, R., O'Regan, M., Stranne, C.,
562 Ananiev, R., Barrientos Macho, N., Cherniykh, D., Coxall, H., Eriksson, B., Floden,
563 T., Gemery, L., Gustafsson, O., Jerram, K., Johansson, C., Khortov, A.,
564 Mohammad, R., and Semiletov, I.: Evidence for an ice shelf covering the central
565 Arctic Ocean during the penultimate glaciation, *Nature Communications*, 7,
566 doi:10.1038/ncomms10365, 2016.
- 567 Jones, E. P.: Circulation in the Arctic Ocean, *Polar Res*, 20, 139-146, 2001.
- 568 Joy, J. A. and Clark, D.L.: The distribution, ecology and systematics of the benthic
569 Ostracoda of the central Arctic Ocean, *Micropaleontology*, 23, 129–154. 1977.
- 570 Karanovic, I. and Brandão, S. N.: The genus *Polycope* (Polycopidae, Ostracoda) in
571 the North Atlantic and Arctic: taxonomy, distribution, and ecology, *Syst Biodivers*,
572 14, 198-223, 2016.
- 573 Karanovic, I. and Brandão, S. N.: Review and phylogeny of the Recent
574 Polycopidae (Ostracoda, Cladocopina), with descriptions of nine new species, one

575 new genus, and one new subgenus from the deep South Atlantic, *Mar Biodivers*,
576 42, 329-393, 2012.

577 Kaufman, D. S., Axford, Y. L., Henderson, A. C. G., McKay, N. P., Oswald, W. W.,
578 Saenger, C., Anderson, R. S., Bailey, H. L., Clegg, B., Gajewski, K., Hu, F. S.,
579 Jones, M. C., Massa, C., Routson, C. C., Werner, A., Wooller, M. J., and Yu, Z. C.:
580 Holocene climate changes in eastern Beringia (NW North America) - A systematic
581 review of multi-proxy evidence, *Quaternary Sci Rev*, 147, 312-339, 2016.

582 Kaufman, D. S., Ager, T. A., Anderson, N. J., Anderson, P. M., Andrews, J. T.,
583 Bartlein, P. J., Brubaker, L. B., Coats, L. L., Cwynar, L. C., Duvall, M. L., Dyke, A.
584 S., Edwards, M. E., Eisner, W. R., Gajewski, K., Geirsdottir, A., Hu, F. S.,
585 Jennings, A. E., Kaplan, M. R., Kerwin, M. N., Lozhkin, A. V., MacDonald, G. M.,
586 Miller, G. H., Mock, C. J., Oswald, W. W., Otto-Bliesner, B. L., Porinchu, D. F.,
587 Ruhland, K., Smol, J. P., Steig, E. J., and Wolfe, B. B.: Holocene thermal
588 maximum in the western Arctic (0-180 degrees W), *Quaternary Sci Rev*, 23, 529-
589 560, 2004.

590 Laxon, S.W., Giles, K.A., Ridout, A.L., Wingham, D.J., Willatt, R., Cullen, R., Kwok,
591 R., Schweiger, A., Zhang, J., Haas, C., Hendricks, S., Krishfield, R., Kurtz, N.,
592 Farrell, S.L. and Davidson, M.: CryoSat estimates of Arctic sea ice volume,
593 *Geophys Res Lett*, 40, doi:10.1002/grl.50193, 2013.

594 Marzen, R. E., DeNinno, L. H. and Cronin, T. M.: Calcareous microfossil-based
595 orbital cyclostratigraphy in the Arctic Ocean, *Quaternary Sci Rev*, 149, 109-121,
596 2016.

597
598 Moore, G. W. K., Våge, K., Pickart, R. S. and Renfrew, I. A.: Decreasing intensity
599 of open-ocean convection in the Greenland and Iceland seas, *Nature Climate*
600 *Change*, doi: 10.1038/nclimate2688, 2015.

601 National Oceanic and Atmospheric Administration's National Centers for
602 Environmental Information, [https://www.ncdc.noaa.gov/data-](https://www.ncdc.noaa.gov/data-access/paleoclimatology-data/datasets)
603 [access/paleoclimatology-data/datasets](https://www.ncdc.noaa.gov/data-access/paleoclimatology-data/datasets)

604 Neale, J. W. and Howe, H.V.: The marine Ostracoda of Russian Harbour, Novaya
605 Zemlya and other high latitude faunas, *Bulletin of American Paleontology*, 65(282),
606 381-431, 1975.

607 Nørgaard-Pedersen, N., Mikkelsen, N., Lassen, S. J., Kristoffersen, Y., Sheldon,
608 E.: Reduced sea ice concentrations in the Arctic Ocean during the last interglacial
609 period revealed by sediment cores off northern Greenland, *Paleoceanography*, 22,
610 PA1218, doi:10.1029/2006PA001283, 2007.

611 Nørgaard-Pederson, N., Spielhagen, R.F., Erlenkeuser, H., Grootes, P.M.,
612 Heinemeier, J., Knies, J.: Arctic Ocean during the Last Glacial Maximum: Atlantic
613 and polar domains of surface water mass distribution and ice cover,
614 *Paleoceanography*, 18(3), 1063, doi:10.1029/2002PA000781, 2003.

- 615 Olsson, K. and Anderson, L.G.: Input and biogeochemical transformation of
616 dissolved carbon in the Siberian shelf seas, *Cont Shelf Res*, 17(7), 819–833, 1997.
- 617 O'Regan, M.: Late Cenozoic paleoceanography of the central Arctic Ocean. *IOP*
618 *Conf. Series: Earth and Environmental Science* 14, doi:10.1088/1755-
619 1315/14/1/012002, 2011.
- 620
621 O'Regan, M., Moran, K., Backman, J., Jakobsson, M., Sangiorgi, F., Brinkhuis, H.,
622 Pockalny, R., Skelton, A., Stickley, C., Koc, N., Brumsack, H. J., and Willard, D.:
623 Mid-Cenozoic tectonic and paleoenvironmental setting of the central Arctic Ocean,
624 *Paleoceanography*, 23, 2008.
- 625
626 Pearce, C., A. Varhelyi, S. Wastegård, F. Muschitiello, N. Barrientos, M. O'Regan,
627 T. M. Cronin, L. Gemery, I. Semiletov, J. Backman, M. Jakobsson: The 3.6 ka
628 Aniakchak tephra in the Arctic Ocean: a constraint on the Holocene radiocarbon
629 reservoir age in the Chukchi Sea, *Climate of the Past*, 2017, doi:10.5194/cp-2016-
630 112, 2017.
- 631
632 Penney, D.N.: Late Pliocene to Early Pleistocene ostracod stratigraphy and
633 palaeoclimate of the Lodin Elv and Kap Kobenhavn formations, East Greenland,
634 *Palaeogeogr, Palaeoclimatol, Palaeoecol*, 101, 49-66, 1993.
- 635
636 Penney, D.N.: Quaternary ostracod chronology of the central North Sea: The
637 record from BH 81/29, *Courier Forschungs-Institut Senckenberg*, 123, 97-109,
1990.
- 638
639 Poirier, R. K., Cronin, T. M., Briggs, W. M. and Lockwood, R.: Central Arctic
640 paleoceanography for the last 50 kyr based on ostracode faunal assemblages, *Mar*
Micropaleontol, 101, 194-194, 2012.
- 641
642 Polyak, L., Bischof, J., Ortiz, J., Darby, D., Channell, J., Xuan, C., Kaufman, D.,
643 Lovlie, R., Schneider, D., Adler, R.: Late Quaternary stratigraphy and
644 sedimentation patterns in the western Arctic Ocean, *Global Planet Change*, 68,5–
17, 2009.
- 645
646 Polyak, L.V.: New data on microfauna and stratigraphy of bottom sediments of the
647 Mendelev Ridge, Arctic Ocean. In: Andreev, S.I. (Ed.), *Sedimentogenes i*
648 *konkrecoobrazovanie v okeane (Sedimentogenesis and nodule-formation in the*
Ocean). *Sevmorgeologia, Leningrad*, 40-50 (in Russian), 1986.
- 649
650 Polyak, L., Curry, W. B., Darby, D. A., Bischof, J., and Cronin, T. M.: Contrasting
651 glacial/interglacial regimes in the western Arctic Ocean as exemplified by a
652 sedimentary record from the Mendelev Ridge, *Palaeogeogr, Palaeocl*, 203, 73-
93, 2004.
- 653
654 Polyak, L., Alley, R.B., Andrews, J.T., Brigham-Grette, J., Darby, D., Dyke, A.,
655 Fitzpatrick, J.J., Funder, S., Holland, M., Jennings, A., Miller, G.H., Savelle, J.,
656 Serreze, M., White, J.W.C. and Wolff, E.: History of Sea Ice in the Arctic,
Quaternary Sci Rev, 29, 1757-1778, 2010.

- 657 Polyakov, I. V., Pnyushkov, A.V., Alkire, M.B., Ashik, I. M., Baumann, T.M.,
658 Carmack, E. C., Goszczko, I., Guthrie, J., Ivanov, V.V., Kanzow, T., Krishfield, R.,
659 Kwok, R., Sundfjord, A., Morison, J., Rember, R., Yulin, A. Greater role for Atlantic
660 inflows on sea-ice loss in the Eurasian Basin of the Arctic Ocean, *Science*, 356,
661 285–291, doi: 10.1126/science.aai8204, 2017.
- 662 Rabe, B., Karcher, M., Schauer, U., Toole, J.M., Krishfield, R.A., Pisarev, S.,
663 Kauker, F., Gerdes, R., Kikuchi, T.: An assessment of Arctic Ocean freshwater
664 content changes from the 1990s to the 2006–2008 period. *Deep Sea Research*
665 *Part I: Oceanographic Research Papers*, 58(2), 173, doi:
666 [10.1016/j.dsr.2010.12.002](https://doi.org/10.1016/j.dsr.2010.12.002), 2011.
- 667 Raup, D.M.: The future of analytical paleobiology, In: Gilinsky, N.L., Signor, P.W.
668 (Eds.), *Analytical Paleobiology: Paleontological Society Short Courses in*
669 *Paleontology*, 4, 207–216, 1991.
- 670 Reimer, P. J. and Reimer, R. W.: A marine reservoir correction database and on-
671 line interface, *Radiocarbon*, 43(2A), 461–463, doi:10.2458/azu_js_rc.43.3986,
672 2001.
673
- 674 Reimer, P. J., Bard, E., Bayliss, A., Beck, J. W., Blackwell, P. G., Bronk Ramsey,
675 C., Grootes, P. M., Guilderson, T. P., Hafliðason, H., Hajdas, I., Hatté, C., Heaton,
676 T. J., Hoffmann, D. L., Hogg, A. G., Hughen, K. A., Kaiser, K. F., Kromer, B.,
677 Manning, S. W., Niu, M., Reimer, R. W., Richards, D. A., Scott, E. M., Southon, J.
678 R., Staff, R. A., Turney, C.S.M. and Plicht, J. van der: IntCal13 and Marine13
679 Radiocarbon Age Calibration Curves 0–50,000 Years cal BP, *Radiocarbon*, 55(4),
680 1869–1887, doi:10.2458/azu_js_rc.55.16947, 2013.
- 681 Repenning, C.A., Brouwers, E.M., Carter, L.D., Marincovich Jr., L. and Ager, T.A.:
682 The Beringian ancestry of *Phenacomys* (Rodentia: Cricetidae) and the beginning
683 of the modern Arctic Ocean Borderland biota, *U.S. Geological Survey Bulletin*,
684 1687, 1-31, 1987.
- 685 Rudels, B., Schauer, U., Bjork, G., Korhonen, M., Pisarev, S., Rabe, B. and
686 Wisotzki, A.: Observations of water masses and circulation with focus on the
687 Eurasian Basin of the Arctic Ocean from the 1990s to the late 2000s, *Ocean Sci*, 9,
688 147-169, 2013.
- 689 Rudels, B.: Arctic Ocean circulation and variability - advection and external forcing
690 encounter constraints and local processes, *Ocean Sci*, 8, 261-286, 2012.
- 691 Schornikov, E. I.: *Acetabulastoma*—a new genus of ostracodes, ectoparasites of
692 *Amphipoda*, *Zoologicheskyy Zhurnal*, (in Russian), 49, 132–1143, 1970.
- 693 Scott, D. B., Schell, T., St-Onge, G., Rochon, A., and Blasco, S.: Foraminiferal
694 assemblage changes over the last 15,000 years on the Mackenzie-Beaufort Sea
695 Slope and Amundsen Gulf, Canada: Implications for past sea ice conditions,
696 *Paleoceanography*, 24, 2009.

- 697 Serreze M.C. and Stroeve J.: Arctic sea ice trends, variability and implications for
 698 seasonal ice forecasting, *Philosophical transactions Series A, Mathematical,*
 699 *physical, and engineering sciences*, 373(2045), 20140159.
 700 doi:10.1098/rsta.2014.0159, 2015.
- 701 Siddiqui, Q.A.: The Iperk Sequence (Plio-Pleistocene) and its Ostracod
 702 Assemblages in the Eastern Beaufort Sea. In: T. Hanai, N. Ikeya and K. Ishizaki
 703 (eds.), *Evolutionary Biology on Ostracoda*, Proc. Ninth Int Symp Ostracoda,
 704 Kodansha, Tokyo, pp. 533-540, 1988.
- 705 Smedsrud, L. H., Halvorsen, M. H., Stroeve, J. C., Zhang, R., and Kloster, K.:
 706 Fram Strait sea ice export variability and September Arctic sea ice extent over the
 707 last 80 years, *The Cryosphere*, 11, 65-79, doi:10.5194/tc-11-65-2017, 2017.
- 708 Somavilla, R., Schauer, U. and Budeus, G.: Increasing amount of Arctic Ocean
 709 deep waters in the Greenland Sea, *Geophys Res Lett*, 40, 4361-4366, 2013.
- 710 Spielhagen, R. F., Baumann, K. H., Erlenkeuser, H., Nowaczyk, N. R., Norgaard-
 711 Pedersen, N., Vogt, C., and Weiel, D.: Arctic Ocean deep-sea record of northern
 712 Eurasian ice sheet history, *Quaternary Sci Rev*, 23, 1455-1483, 2004.
 713
- 714 Stein, R. , Fahl, K. and Müller, J.: Proxy reconstruction of Arctic Ocean sea ice
 715 history - From IRD to IP25 , *Polarforschung*, 82, 37-71, 2012.
 716
- 717 Stepanova, A., Taldenkova, E., Bauch, H.A.: Late Saalian–Eemian ostracods from
 718 the northern White Sea region, *Joannea Geol Paläont*, 11, 196-198 (abstract only),
 719 2011.
- 720 Stepanova, A. Y., Taldenkova, E. E., Bauch, H. A.: Arctic quaternary ostracods
 721 and their use in paleoreconstructions, *Paleontol J+*, 44, 41-48, 2010.
- 722 Stepanova, A., Taldenkova, E., Simstich, J., Bauch, H.A.: Comparison study of the
 723 modern ostracod associations in the Kara and Laptev seas: Ecological aspects,
 724 *Marine Micropaleontology*, 63, 111-142, 2007.
- 725 Stepanova, A. Y.: Late Pleistocene-Holocene and Recent Ostracoda of the Laptev
 726 Sea and their importance for paleoenvironmental reconstructions, *Paleontol J+*, 40,
 727 S91-S204, 2006.
- 728 Stepanova, A., Taldenkova, E., Bauch, H.A.: Recent Ostracoda of the Laptev Sea
 729 (Arctic Siberia): taxonomic composition and some environmental implications,
 730 *Marine Micropaleontology*, 48(1-2), 23-48, 2003.
- 731 Stroeve, J. C., Markus, T., Boisvert, L., Miller, J. and Barrett, A.: Changes in Arctic
 732 melt season and implications for sea ice loss, *Geophys Res Lett*, 41(4),
 733 2013GL058951, doi:10.1002/2013GL058951, 2014.

- 734 Stroeve, J. C., Serreze, M. C., Holland, M. M., Kay, J. E., Malanik, J. and Barrett, A.
735 P.: The Arctic's rapidly shrinking sea ice cover: a research synthesis, *Climatic*
736 *Change*, 110, 1005-1027, 2012.
- 737 Stuiver, M., Reimer, P.J., and Reimer, R.W.: CALIB 7.1 [WWW program] at
738 <http://calib.org>, 2010.
- 739 SWERUS C3 2014 Expedition. The Swedish –Russian – US Arctic Ocean
740 Investigation of Climate-Cryosphere-Carbon Interactions – The SWERUS-C3 2014
741 Expedition Cruise Report Leg 2 (of 2)
742 (<ftp://ftp.geo.su.se/martinj/outgoing/SWERUSC3/Leg2%20Cruise%20Report/>).
- 743 Taldenkova, E., Bauch, H. A., Stepanova, A., Ovsepyan, Y., Pogodina, I.,
744 Klyuvitkina, T., and Nikolaev, S.: Benthic and planktic community changes at the
745 North Siberian margin in response to Atlantic water mass variability since last
746 deglacial times, *Mar Micropaleontol*, 96-97, 13-28,
747 doi:10.1016/j.marmicro.2012.06.007, 2012.
- 748 Taldenkova, E., Bauch, H.A., Stepanova, A., Strezh, A., Dem'yankov, S.,
749 Ovsepyan, Ya., Postglacial to Holocene benthic assemblages from the Laptev
750 Sea: paleoenvironmental implications, *Quaternary International*, 183, 40–60, 2008.
- 751 Taldenkova, E., Bauch, H. A., Stepanova, A., Dem'yankov, S. and Ovsepyan, A.:
752 Last postglacial environmental evolution of the Laptev Sea shelf as reflected in
753 molluscan, ostracodal, and foraminiferal faunas, *Global Planet Change*, 48, 223-
754 251, 2005.
- 755 Wassmann, P., Duarte, C. M., Agusti, S., and Sejr, M. K.: Footprints of climate
756 change in the Arctic marine ecosystem, *Global Change Biol*, 17, 1235-1249, 2011.
- 757 Whatley, R., Eynon, M. and Moguilevsky, A.: The depth distribution of Ostracoda
758 from the Greenland Sea, *Journal of Micropalaeontology*, 17, 15–32, 1998.
- 759 Whatley, R. C., Eynon, M. P. and Moguilevsky, A.: Recent Ostracoda of the
760 Scoresby Sund Fjord system, East Greenland, *Revista Española de*
761 *Micropaleontologia*, 28(2), 5-23, 1996.
- 762 Wollenburg, J. E., Kuhnt, W., and Mackensen, A.: Changes in Arctic Ocean
763 paleoproductivity and hydrography during the last 145 kyr: The benthic
764 foraminiferal record, *Paleoceanography*, 16, 65-77, 2001.
- 765 Xiao, X., Stein, R., Fahl, K.: MIS 3 to MIS 1 temporal and LGM spatial variability in
766 Arctic Ocean sea ice cover: Reconstruction from biomarkers, *Paleoceanography*,
767 30, doi:10.1002/2015PA002814, 2015.
- 768 Yasuhara, M., Stepanova, A., Okahashi, H., Cronin, T.M. and Brouwers, E.M.:
769 Taxonomic revision of deep-sea Ostracoda from the Arctic Ocean,
770 *Micropaleontology*, 60, 399-444, 2014.

771 Zarijian, C. A. A., Stepanova, A. Y., and Grutzner, J.: Glacial-interglacial variability
 772 in deep sea ostracod assemblage composition at IODP Site U1314 in the subpolar
 773 North Atlantic, *Mar Geol*, 258, 69-87, 2009.

774 Zemp, M., Frey, H., Gartner-Roer, I., Nussbaumer, S. U., Hoelzle, M., Paul, F.,
 775 Haeberli, W., Denzinger, F., Ahlstrom, A. P., Anderson, B., Bajracharya, S.,
 776 Baroni, C., Braun, L. N., Caceres, B. E., Casassa, G., Cobos, G., Davila, L. R.,
 777 Granados, H. D., Demuth, M. N., Espizua, L., Fischer, A., Fujita, K., Gadek, B.,
 778 Ghazanfar, A., Hagen, J. O., Holmlund, P., Karimi, N., Li, Z. Q., Pelto, M., Pitte, P.,
 779 Popovnin, V. V., Portocarrero, C. A., Prinz, R., Sangewar, C. V., Severskiy, I.,
 780 Sigurosson, O., Soruco, A., Usubaliev, R., Vincent, C., and Correspondents, W.
 781 N.: Historically unprecedented global glacier decline in the early 21st century, *J*
 782 *Glaciol*, 61, 745-+, 2015.

Table 1. Expedition and core site data for cores presented in this study.

Year	Expedition	Core name	Latitude	Longitude	Water depth (m)	Location
2014	SWERUS-L2	SWERUS-L2-32-MC4	85.14	151.59	837	Lomonosov Ridge
2014	SWERUS-L2	SWERUS-L2-32-GC2	85.15	151.66	828	Lomonosov Ridge
2014	SWERUS-L2	SWERUS-L2-24-MC4	78.80	165.38	982	E. Siberian Sea Slope
2014	SWERUS-L2	SWERUS-L2-28-MC1	79.92	154.35	1145	E. Siberian Sea Slope
2014	SWERUS-L2	SWERUS-L2-33-TWC1	84.28	148.65	888	Lomonosov Ridge
2014	SWERUS-L2	SWERUS-L2-34-MC4	84.28	148.71	886	Lomonosov Ridge
1994	AOS SR96-1994	PI-94-AR-BC28	88.87	140.18	1990	Lomonosov Ridge
1991	Arctic 91	PS 2179-3 MC	87.75	138.16	1228	Lomonosov Ridge
1991	Arctic 91	PS 2185-4 MC	87.53	144.48	1051	Lomonosov Ridge
1994	AOS SR96-1994	PI-94-AR-BC8	78.13	176.75	1031	Mendeleev Ridge
1994	AOS SR96-1994	PI-94-AR-BC12A	79.99	174.29	1683	Mendeleev Ridge
2005	HOTRAX	HLY0503-6	78.29	-176.99	800	Mendeleev Ridge
1994	AOS SR96-1994	P1-94-AR-PC10	78.15	-174.63	1673	Mendeleev Ridge
1992	USGS-Polar Star	P1-92-AR-P40	76.26	-157.55	700	Northwind Ridge
1992	USGS-Polar Star	P1-92-AR-P30	75.31	-158.05	765	Northwind Ridge
2007	LOMROG 07	LOMROG07-PC-04	86.70	-53.77	811	Lomonosov Ridge
1996	Oden 96	96-12-1PC	87.10	144.77	1003	Lomonosov Ridge

Table 2. Radiocarbon dates for SWERUS 32 cores, uncalibrated ^{14}C age and calibrated ^{14}C chronology.

32-MC/GC chronology		Unmodelled 2 sigma (2 std dev)				Modelled 2 sigma (2 std dev)			
Lab number (^{14}C date age, error)	Depth (cm)	from	to	mean	error	from	to	mean**	error
OS-124799 (3410, 25)	2.5	3168	2698	2912	124	3045	2605	2802	105
OS-124798 (6110, 20)	4.5	6435	5974	6213	116	6317	5902	6140	113
OS-124599 (7920, 35)	5.5	8313	7874	8085	110	8176	7766	7972	101
OS-124598 (8290, 30)	8.5	8715	8207	8465	119	8576	8187	8385	99
OS-124597 (11000, 35)	11.5	12525	11661	12094	222	12191	11353	11831	230
OS-124754 (11200, 40)	14.5	12635	12040	12365	164	12625	12008	12381	165

OS-125185 (18650, 80)	19.5	22116	21357	21729	183	21973	21252	21637	179
OS-125190 (29400, 280)	24.5	33567	31805	32733	462	33298	31585	32423	455
OS-125192 (35400, 560)	31.5	40705	38099	39301	638	40858	38451	39608	608
OS-127484 (40000, 1700)	33*	47589	40881	43837	1646	44472	40403	42428	1002

All ages as calibrated years BP

$\Delta R = 300 \pm 100$ years (Reimer and Reimer, 2001)

Marine13 calibration curve (Reimer et al., 2013)

*Sample collected from 32-GC, original depth was 36 cm but corrected by 3 cm based on ostracode correlation with 32-MC

**We used the modeled, mean, 2-sigma age to plot species' relative frequencies.

Table 3. List of species included in genus-level groups.

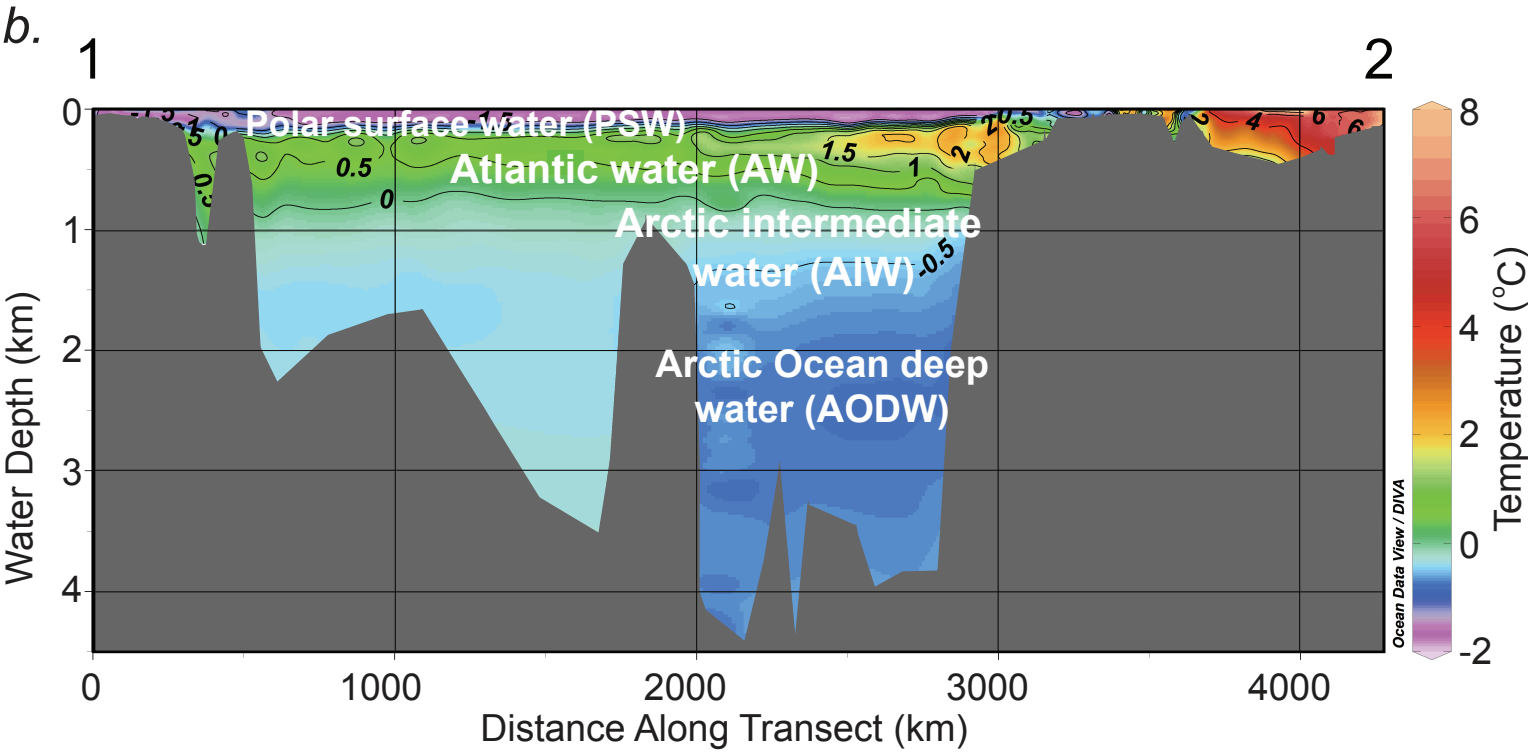
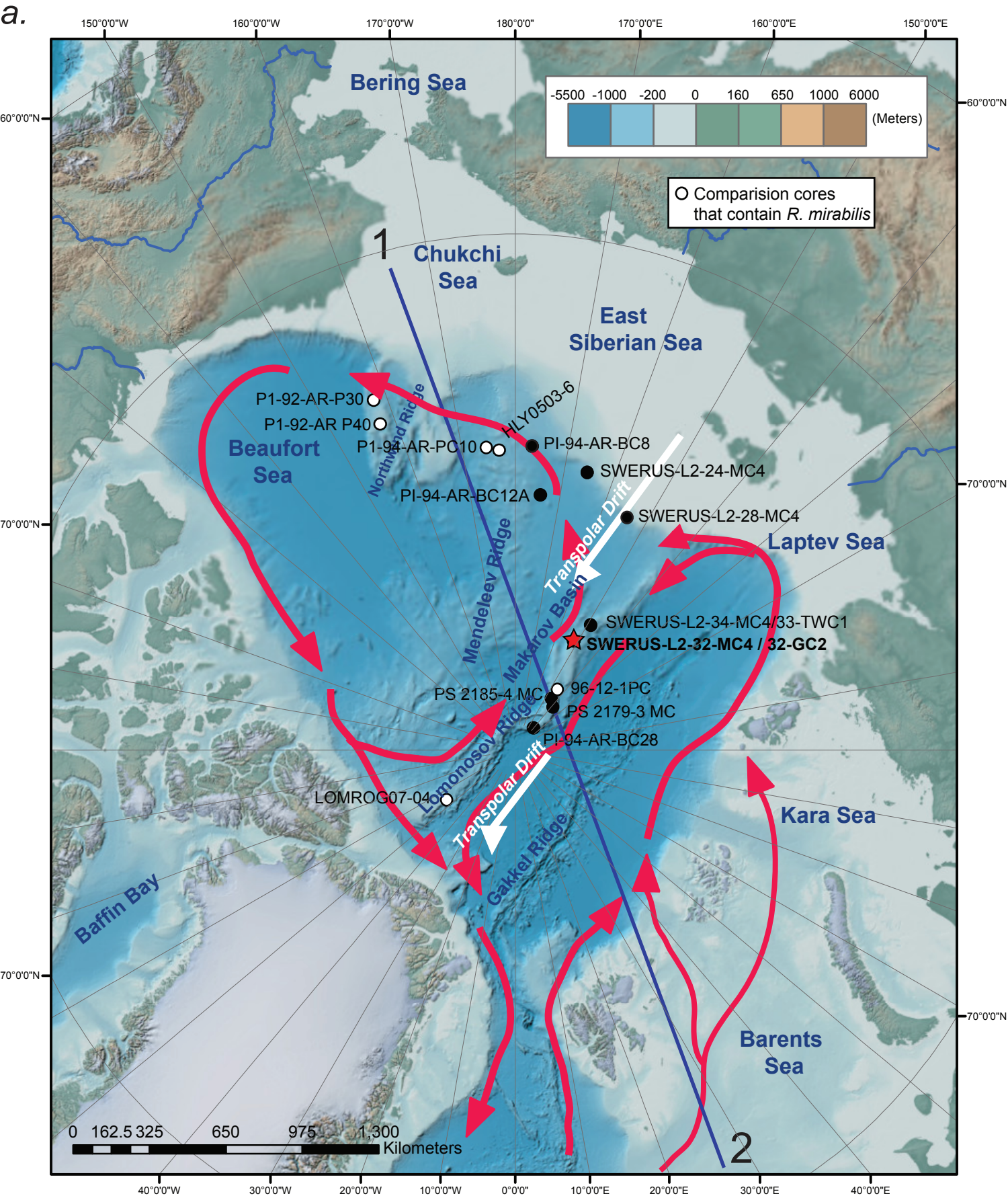
Group name	Species included in Group:
<i>Cytheropteron</i> spp.	<i>Cytheropteron higashikawai</i> Ishizaki 1981, <i>Cytheropteron scoresbyi</i> Whatley and Eynon 1996, <i>Cytheropteron sedovi</i> Schneider 1969 and <i>Cytheropteron parahamatum</i> Yasuhara, Stepanova, Okahashi, Cronin and Brouwers 2014.
<i>Polycopse</i> spp.	<i>P. inornata</i> Joy & Clark, 1977 and <i>P. bireticulata</i> Joy & Clark, 1977. (For scanning electron microscope images, see Joy & Clark 1977: Plate 3, Fig. 1; Yasuhara et al., 2014: Plate 3, Figs 2-5 and Plate 2, Figs 1-2.) May include: <i>P. arcys</i> (Joy & Clark, 1977), <i>P. punctata</i> (Sars 1869), <i>P. bispinosa</i> Joy & Clark 1977, <i>P. horrida</i> Joy & Clark 1977, <i>P. moenia</i> Joy & Clark 1977, <i>P. semipunctata</i> Joy & Clark 1977, <i>P. obicularis</i> Sars 1866. <i>P. pseudoinornata</i> Chavtur, 1983 and <i>P. reticulata</i> Muller 1894

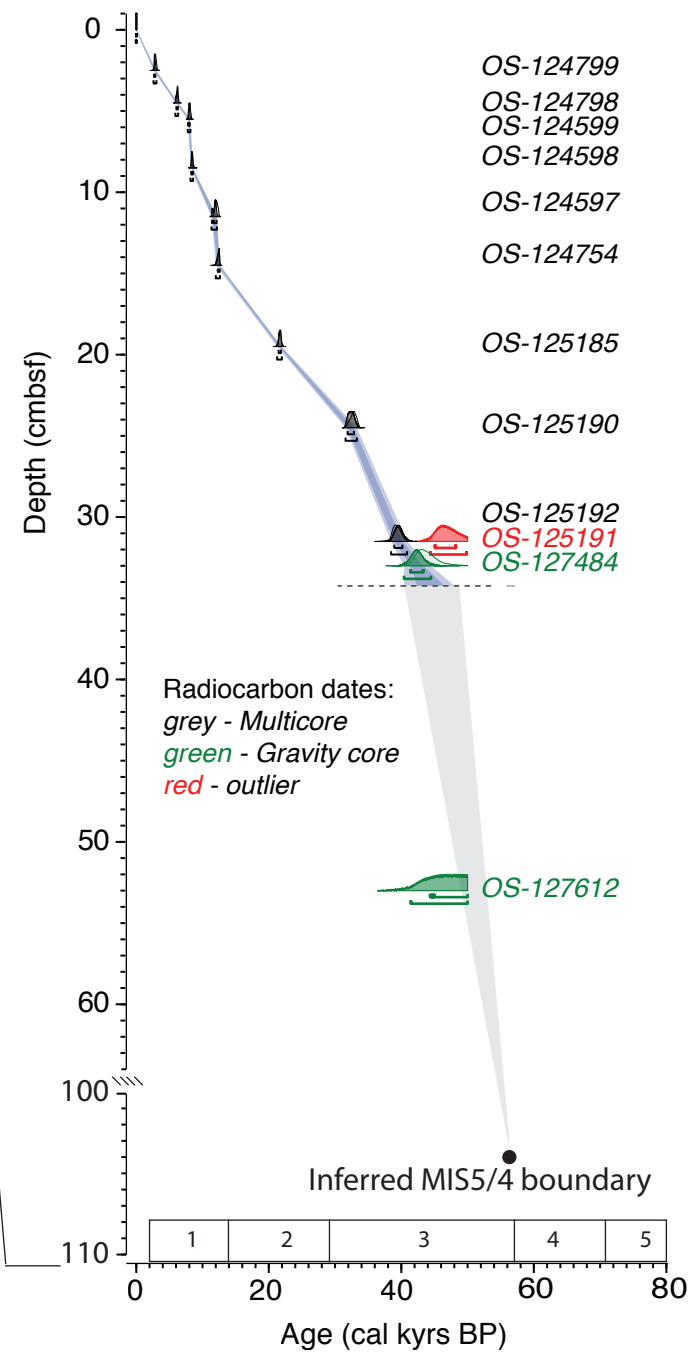
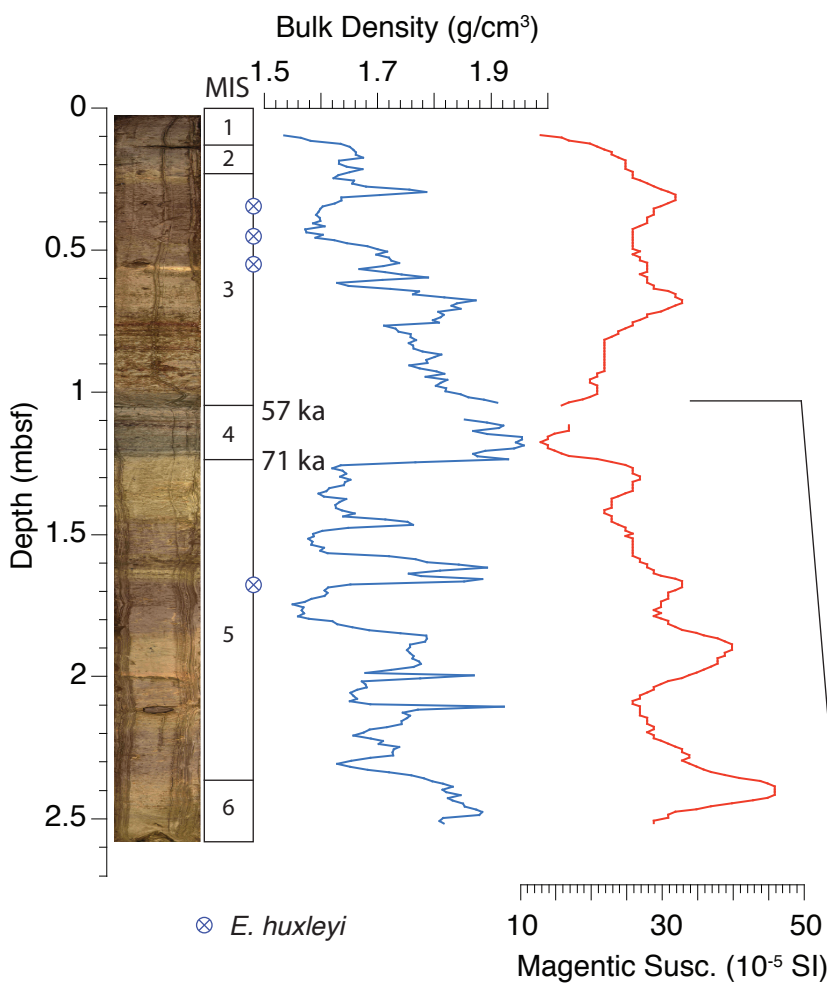
Table 4. Summary of indicator species, pertinent aspects of their modern ecology and paleoenvironmental significance.

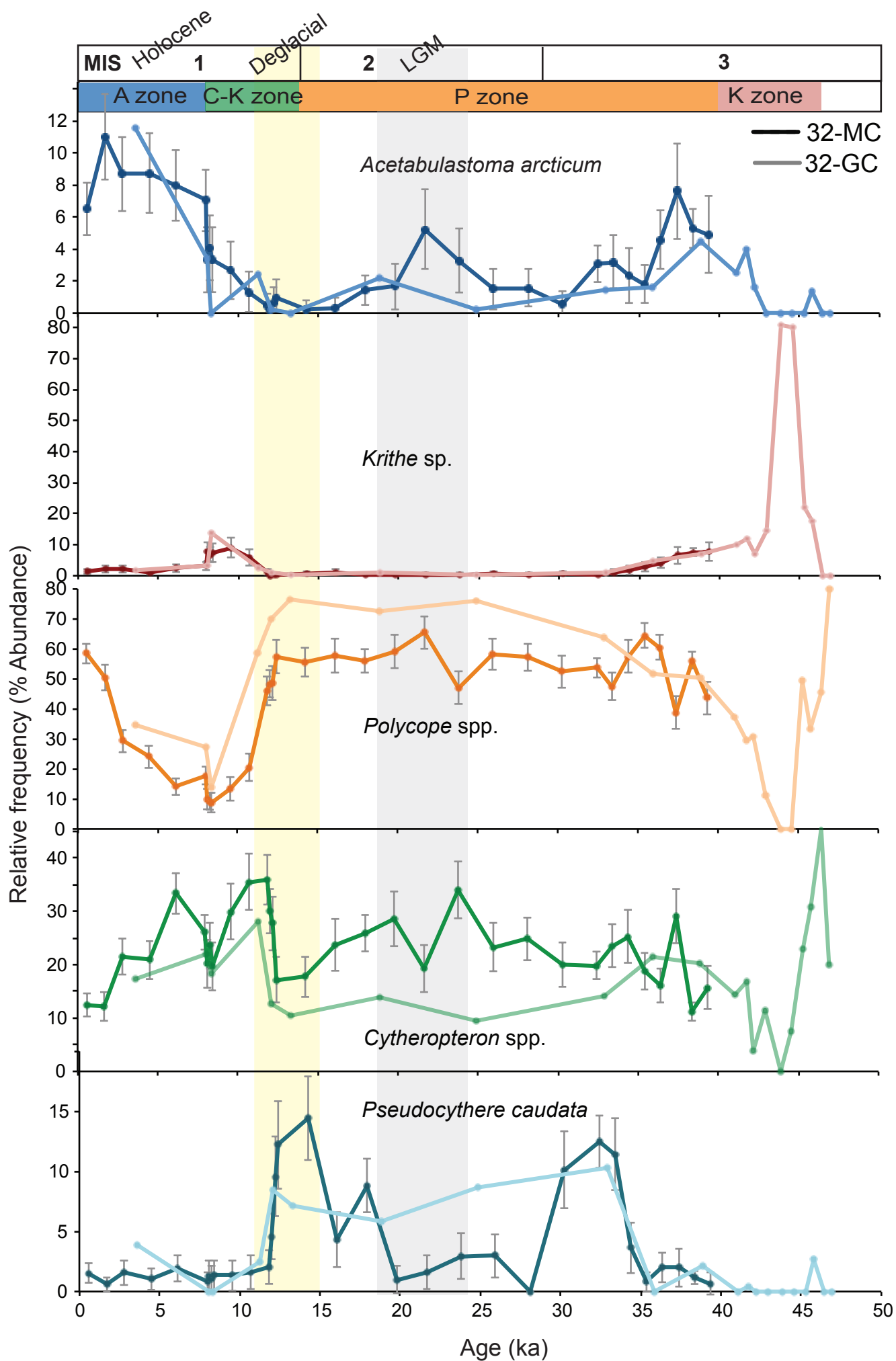
Species	Modern ecology / paleoenvironmental significance
<i>Acetabulastoma arcticum</i> (Schornikov, 1970)	The stratigraphic distribution of <i>A. arcticum</i> is used as an indicator of periods when the Arctic Ocean experienced thicker sea-ice conditions but not fully glacial conditions when productivity would have halted. This pelagic ostracode is a parasite on <i>Gammarus</i> amphipods that live under sea ice in modern, perennially sea-ice-covered regions in the Arctic (Schornikov, 1970). Cronin et al. (2010) used <i>A. arcticum</i> 's presence in 49 late Quaternary Arctic sediment cores as a proxy to reconstruct the Arctic Ocean's sea-ice history during the last ~45 ka.
<i>Krithe</i> spp.	Species of the genus <i>Krithe</i> typically occur in low-nutrient habitats spanning across a range of cold, interstadial temperatures but are especially characteristic of AODW (Cronin et al., 1994; 1995; 2014). In SWERUS-32 cores, <i>K. hunti</i> was far more prevalent than <i>K. minima</i> . From a modern depth-distribution analysis using AOD, <i>K. hunti</i> appears in greatest abundance (50-80% of the assemblage) at depths between 2000-4400 mwd, however, this taxon is also found in significant numbers (20-50%) at depths between 400-2000 m. With a preference for deeper, cold, well-ventilated depths, <i>Krithe</i> spp. events are useful in identifying late Quaternary shifts in Arctic Ocean water masses and making biostratigraphic correlations (Cronin et al., 2014).
<i>Polycope</i> spp.	Today, this Atlantic-derived, myodocopid genus is in highest abundance (40-60% of assemblage) in cold intermediate-depth waters between 800-2300 mwd. It characterizes fine-grained, organic rich sediment in well-oxygenated water. In fossil assemblages, <i>Polycope</i> is indicative of areas with high productivity that are seasonally ice-free or have variable or thin sea-ice cover (Cronin et al., 1995; Poirier et al., 2012).
<i>Cytheropteron</i> spp.	The two dominant <i>Cytheropteron</i> species in 32-MC and 32-GC are <i>C. sedovi</i> and <i>C. scoresbyi</i> , along with lower but significant numbers of <i>C. parahamatum</i> (reaches 24% of assemblage at 10 ka) and <i>C. higashikawai</i> (fluctuates in very low numbers between 0-3% at any given time in downcore samples). These particular <i>Cytheropteron</i> species are broadly diagnostic of deeper, well-ventilated water masses (AIW and AODW).
<i>Pseudocythere caudata</i> Sars 1866	This species of N. Atlantic origin rarely exceeds >15% in modern Arctic Ocean assemblages. It characterizes lower AW and AI water at depths of 1000-2500 mwd. It usually co-occurs with <i>Polycope</i> spp. in fossil assemblages and may be associated with surface conditions (Cronin et al., 1994, 1995, 2014), but more work needs to be done on its ecological significance.

Table 5. Although *R. mirabilis* (Brady, 1868) is known and named from Pleistocene sediments in England and Scotland (Brady et al., 1874), this list cites various workers since that have documented this species in Arctic deposits dating back to the late Pliocene, when summer bottom temperatures were inferred to be up to 4°C warmer than today.

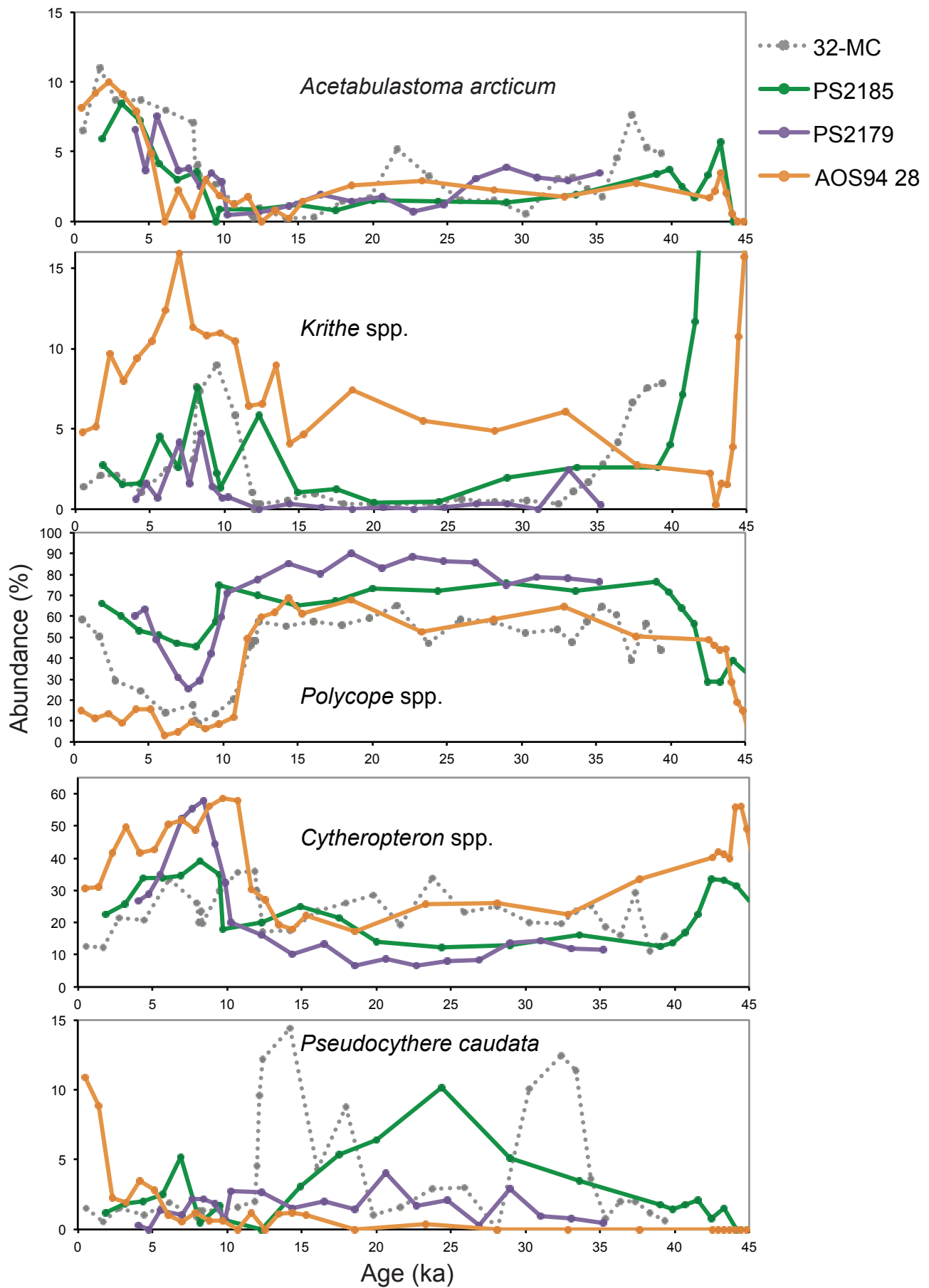
Citation	Location / Formation (Age)
Siddiqui (1988)	Eastern Beaufort Sea's Iperk sequence (Plio-Pleistocene)
Repenning et al. (1987)	Alaska's North Slope Gubik Formation (Pliocene)
Penney (1990)	Central North Sea deposits (early Pleistocene age, 1.0-0.73 Ma)
Feyling-Hassen (1990)	East Greenland's Kap København Formation (late Pliocene)
Penney (1993)	East Greenland's Lodin Elv Formation (late Pliocene)



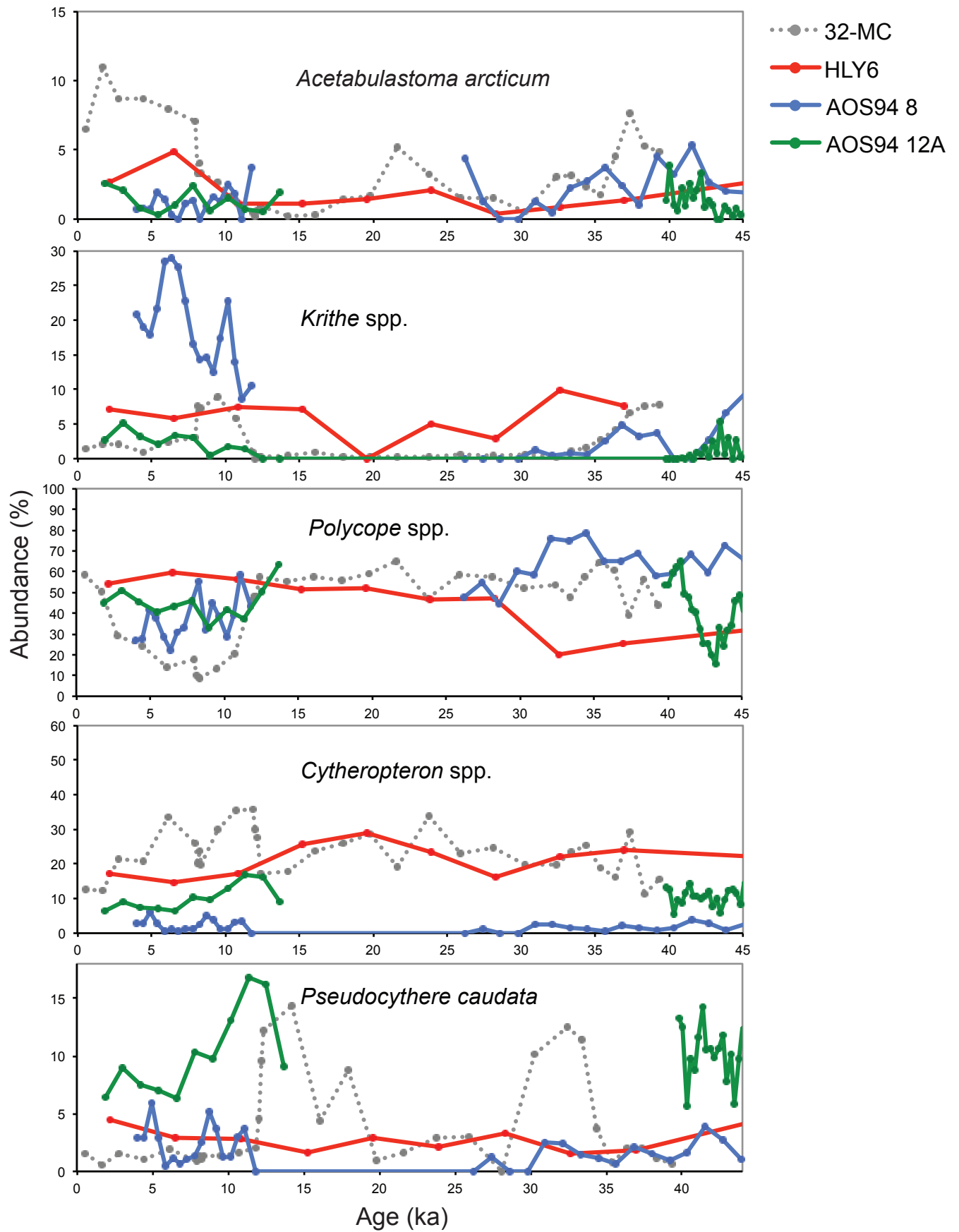




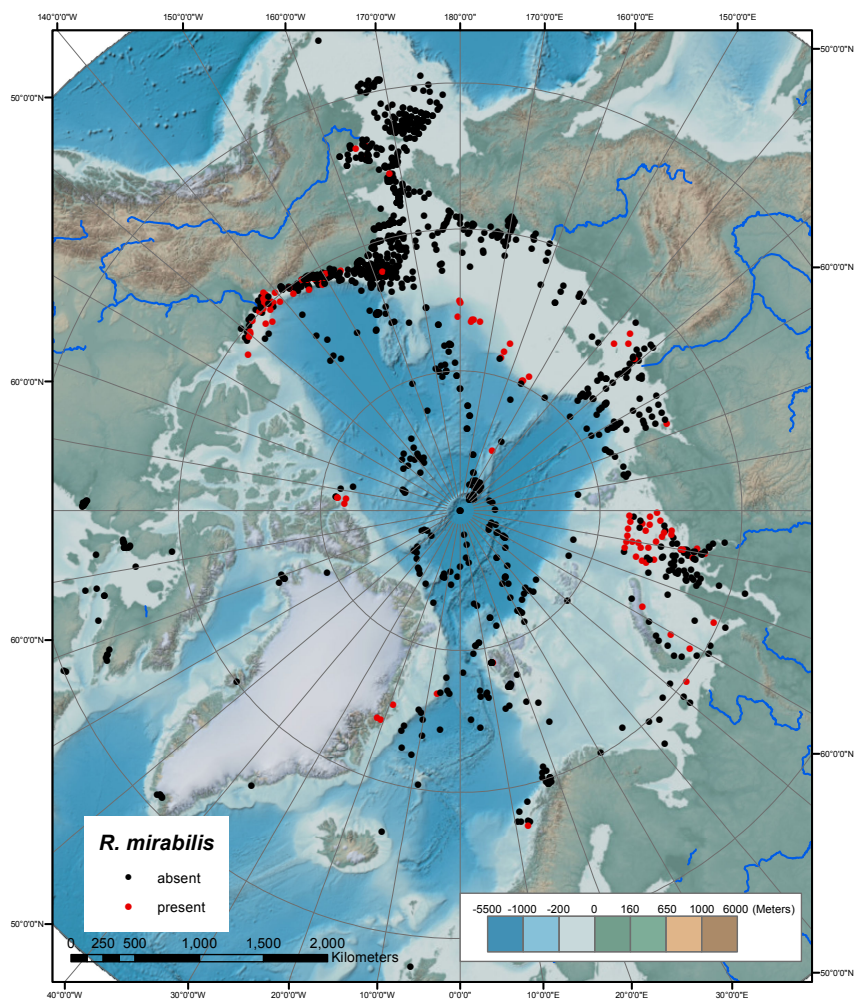
Lomonosov Ridge



Mendeleev Ridge

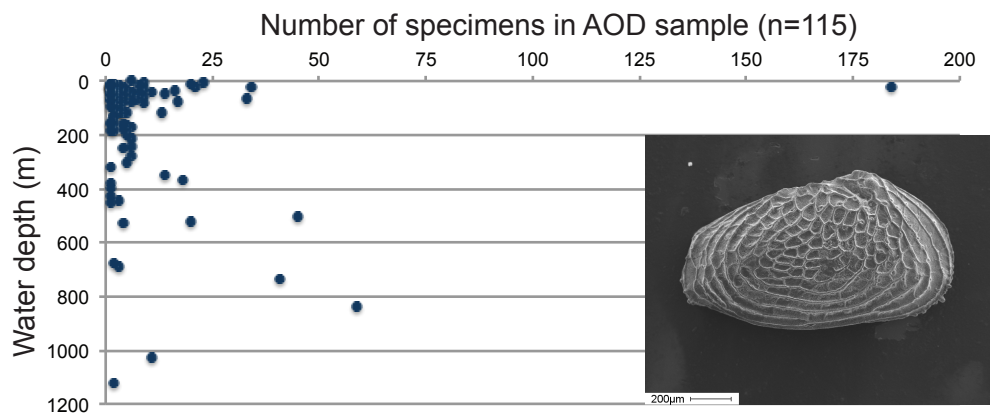


a.

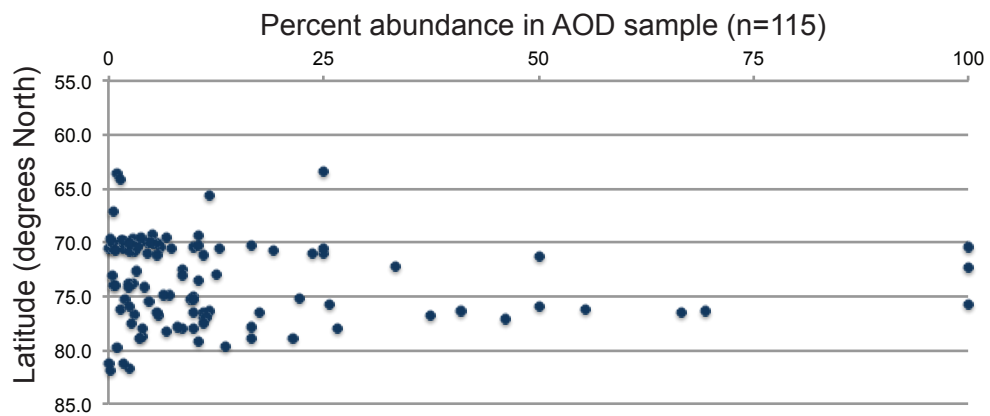


R. mirabilis modern depth and latitude distribution

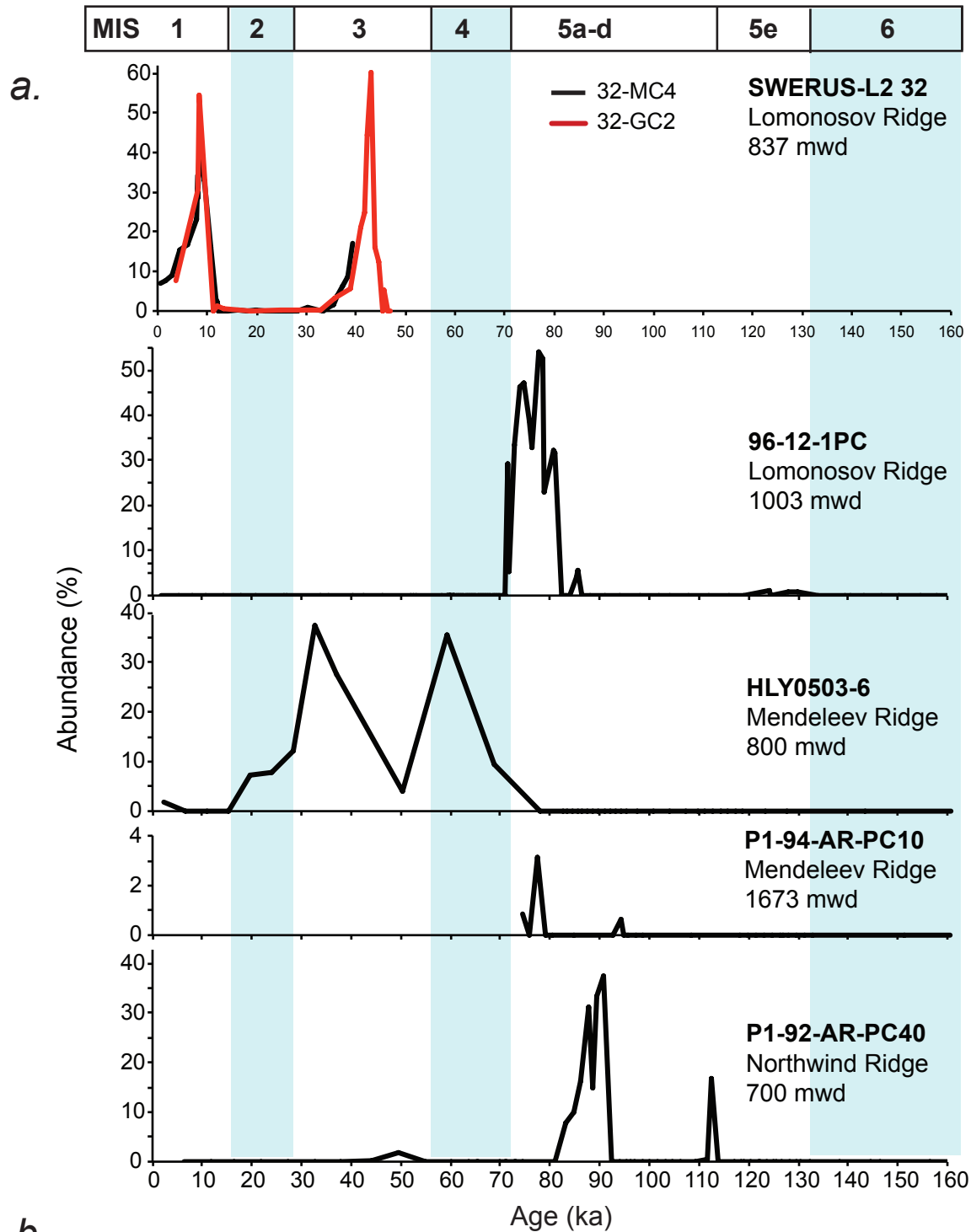
b.



c.



R. mirabilis events



b.

